

## RESEARCH ARTICLE

# Design of Compact and Wideband Groove Gap Waveguide-Based Directional Couplers

MAHDIEH RABBANIFARD<sup>1</sup>, DAVID ZARIFI<sup>1,2</sup>, ALI FARAHBAKHS<sup>2,3</sup>,  
AND MICHAL MROZOWSKI<sup>2</sup>, (Fellow, IEEE)

<sup>1</sup>School of Electrical and Computer Engineering, University of Kashan, Kashan 87317-53153, Iran

<sup>2</sup>Department of Microwave and Antenna Engineering, Faculty of Electronics, Telecommunications and Informatics, Gdańsk University of Technology, 80-233 Gdańsk, Poland

<sup>3</sup>Department of Electrical and Computer Engineering, Graduate University of Advanced Technology, Kerman 76311-33131, Iran

Corresponding author: Davood Zarifi (davood.zarifi@pg.edu.pl)

This work was supported by Gdańsk University of Technology via NOBELIUM through the “Excellence Initiative-Research University” Program under Grant DEC-49/2023/IDUB/I.1 and Grant DEC-50/2023/IDUB/I.1.

**ABSTRACT** This paper proposes a compact cross-shaped groove gap waveguide structure for creating wideband and compact directional couplers with different coupling levels. Groove gap waveguide technology is applied to overcome fabrication challenges of printed and hollow waveguide structures in high frequency bands. The validity of the novel concept is demonstrated through the design and evaluation of several compact broadband directional couplers, featuring 3-, 4.5-, 6-, and 10- dB coupling levels, alongside the fabrication and testing of a compact, wideband 3-dB directional coupler prototype. In addition, an equivalent circuit is proposed to present the behavior of the 3-dB coupler. The comparison of simulation and experimental results for the prototype shows good agreement. The measured transmission coefficients in the output ports are  $-3 \pm 0.5$  dB with a phase imbalance of  $\pm 2.5^\circ$  over 17.9-24 GHz frequency band. The findings confirm the suitability of the proposed directional coupler structure as a compact and self-packaged solution for high-frequency applications.

**INDEX TERMS** Directional coupler, groove gap waveguide, Ka-band applications.

## I. INTRODUCTION

Directional couplers are essential components in microwave and mmWave networks, with diverse applications in communication systems, microwave measurements, and radars. These devices are usually employed for sampling microwave power, monitoring of microwave power and frequency and various applications in measurement setups [1].

Directional couplers can be designed using different technologies including printed circuit boards (PCB) and hollow waveguides. Microstrip couplers are compact and lightweight, and well-suited for seamless integration with both active and passive microwave devices. These couplers with a balanced power split and phase quadrature are required for various applications. Substrate Integrated Waveguide (SIW)-based couplers offer high Q-factors, broad frequency bandwidths, low profiles, and straightforward

fabrication processes [2], [3], [4]. However, both technologies are limited by their low power handling capabilities and significant dielectric losses at higher frequencies. Hollow waveguide-based couplers are usually employed for applications with high power and low loss requirements in mmWave bands. While they outperform PCB-based designs in terms of efficiency, these couplers are larger and heavier. Integrating them with microwave circuits at mmWave frequencies presents challenges, particularly in achieving reliable, reproducible, and low-loss assembly. Ensuring a seamless fit between the microwave circuits and the hollow waveguides is crucial, as any air gaps can lead to increased losses and unwanted resonances.

Over the years, several strategies have been proposed to develop broadband waveguide 3-dB couplers suitable for high-power applications. Typically, these couplers consist of two parallel waveguides positioned closely and interconnected through a series of apertures on either the broader or narrower walls. Multi-section couplers offer the advantage of

The associate editor coordinating the review of this manuscript and approving it for publication was Derek Abbott.

achieving extensive and ultra-wide frequency bandwidth [5]. However, these couplers tend to increase the overall length of the structure due to a substantial number of apertures and the need for considerable spacing. To achieve tight coupling and full bandwidth for 3-dB coupling, these structures often need to span several wavelengths. In [6], a compact 3-dB E-Plane waveguide directional coupler was proposed. This design, which relies on large apertures in the common broadwall of two parallel waveguides, demonstrated high directivity and suitable coupling flatness within the 6.57 to 10 GHz frequency range. More recently, another design featuring a 3-dB E-plane waveguide directional coupler was introduced [7]. That design, operating over the 17.3-20.2 GHz frequency range, demonstrated excellent performance. 3-dB directional couplers, capable of operating across a wide frequency band, can also be implemented as branch-line waveguide structures [8], [9], [10], [11]. For this type of coupler, the coupling region encompasses series branch lines attached to the two neighboring waveguides. The branch-line couplers can be designed for a broad frequency range with an acceptable coupling flatness and 3- to 10-dB coupling values. However, the presence of multiple narrow branch lines often limits the power-handling capabilities and compactness of the design.

Hollow waveguide-based couplers are limited in their applications at high frequencies due to the need for accurate and expensive manufacturing. The main challenge is to achieve an acceptable electrical connection between the different layers. Gap waveguide technology can overcome the limitations of PCB and hollow waveguide technologies [12]. Over the last decades, this technology has been employed to design and implement various high frequency components [13], [14], [15], [16], [17], [18], [19]. Notably, several 3-dB directional couplers have been proposed using printed ridge gap waveguides [20], [21], [22], [23], [24], [25], [26]. In [20], a printed ridge gap waveguide-based 3-dB coupler was presented over the frequency band of 29 to 31 GHz (6% fractional bandwidth) and phase unbalance within  $\pm 10^\circ$ . Another work proposed a broadband 3-dB directional coupler based on printed ridge gap waveguide with 38% fractional bandwidth from 25 GHz to 37 GHz, the phase balance is  $90^\circ \pm 5^\circ$  and an amplitude balance of  $3.4 \pm 0.5$  dB [25]. Briefly, although printed ridge gap waveguides can be fabricated employing a low-cost conventional PCB fabrication process, they cannot meet the requirements of high-power applications.

To ensure good power handling, 3-dB directional couplers based on metal ridge and groove waveguides have been introduced in the literatures [16], [27], [28], [29], [30], and [31]. For instance, in [26], a compact-size hybrid coupler based on a ridge gap waveguide with low insertion loss was proposed. Unfortunately, this design is limited by its narrow bandwidth (14%). In [28], a 3-dB directional coupler was introduced, employing a groove gap waveguide and ensuring continuous coupling between adjacent grooves. While this configuration demonstrated low insertion loss and high isolation, it also suffers from a limited impedance bandwidth of 14% and a

substantial size. Another study proposed a broadband 3-dB directional coupler utilizing a groove gap waveguide, covering a frequency range from 57 to 74 GHz with a bandwidth of 25% and power-split unbalance within  $\pm 0.5$  dB [29]. Additionally, in [31], a 3-dB branch-line coupler was presented based on a ridge gap waveguide across the frequency band of 12 to 20 GHz, but its relatively large size poses a significant challenge.

In light of the points discussed, this paper introduces a novel structure based on gap waveguides for the development of compact, wideband directional couplers with desired coupling levels. A cross-shaped coupling region, derived from a groove gap waveguide, is employed to circumvent fabrication challenges in high frequency bands. By adjusting the dimensions and placement of six tuning pins within the coupling area, it is feasible to achieve the desired coupling level and broadband operation while maintaining a compact footprint. The application of the proposed cross-shaped groove gap waveguide structure for creating wideband and compact directional couplers with different coupling levels is illustrated through the design of four broadband couplers featuring 3-, 4.5-, 6-, and 10-dB coupling levels. To further substantiate the validity of the concept, an equivalent circuit is proposed and a prototype compact 3-dB directional coupler is developed, fabricated and measured with a fractional bandwidth of around 30% centered at 21 GHz, a phase imbalance of  $\pm 2.5^\circ$ , and a coupling of  $3 \pm 0.5$  dB in Ka-band. Compared with other ridge and groove gap waveguide-based 3-dB directional couplers, the proposed coupler exhibits good bandwidth and performance with a compact coupling region with size of  $1.2 \lambda_g \times 1.2 \lambda_g$ .

The present paper is organized as follows: Section II outlines the procedure for determining the dimensions of the groove gap waveguide structure. Section III and IV present the design procedure for the proposed coupler and demonstrates the design of several compact broadband directional couplers with 3-, 4.5-, 6-, and 10-dB coupling levels. Section VI provides measurement results for the fabricated 3dB coupler and compares the performance of several reported 3-dB couplers with the present work.

## II. GAP WAVEGUIDE TECHNOLOGY

The gap waveguide technology uses a parallel-plates waveguide to control the propagation of an electromagnetic wave. In this setup, one plate serves as a perfect electric conductor and the other as a texture featuring periodic pins, aimed at generating a stop-band, to prevent the energy leakage. The unit cell of periodic pins structure is displayed in Fig. 1(a). A guiding structure can be achieved by inserting a groove or ridge into the pin layer, to control electromagnetic wave propagation in the air gap between the layers. The primary benefit of this technology is the ability to create guiding structures without any contact between the layers. By manipulating the geometric parameters of the structure, it is possible to attain the intended stop-band. As described in [12], to ensure a stop-band coverage of 15-25 GHz, appropriate values for the

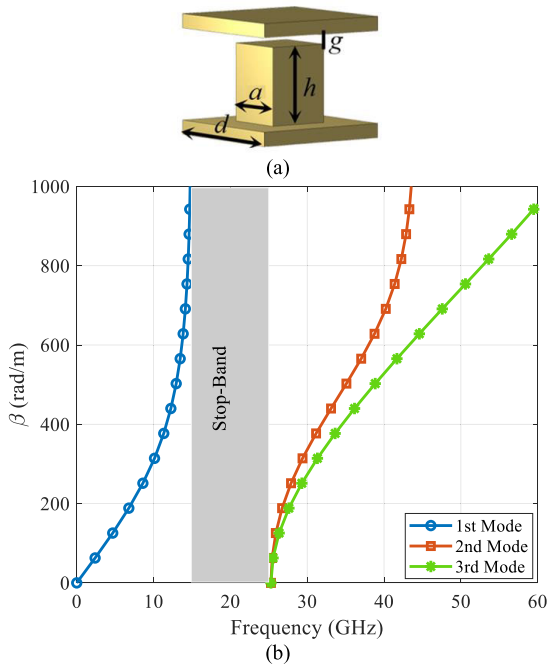


FIGURE 1. (a) unitcell of periodic pin structure. (b) Dispersion diagram for the first three modes.

geometrical parameters are:  $g = 0.75$  mm,  $a = 1.5$  mm,  $p = 1.2$  mm, and  $h = 4.5$  mm. The dispersion diagram of the periodic pins structure is shown in Fig. 1(b).

### III. DESIGN OF CROSS-SHAPED COUPLER

#### A. 3-dB DIRECTIONAL COUPLER

Fig. 2 presents the configuration of the presented cross-shaped 3-dB directional coupler based on groove gap waveguides. This coupler consists of four groove gap waveguides arranged in two rows of periodic pins along the side walls. In this structure, port 1 is excited to distribute the power between the two output ports (2 and 3) and isolate port 4. To attain the targeted 3-dB coupling level between the input and output ports while reducing reflections at the input port, six tuning pins have been placed in the coupling region. The coupler's geometrical parameters are illustrated in Fig. 2(b). Despite apparent multitude of design variables (six pins, each characterized by four – pins 1 through 4, or three – pins 5 and 6, geometry parameters), it is noteworthy to observe that for the 3-dB coupling, the structure has to show symmetry. Accordingly, the dimensions (both width and height) and positions of pins 1 through 4 in the groove gap waveguides linked to the coupling area are consistent. The same consistency applies to pins 5 and 6. Therefore, only seven parameters  $x_1 (= y_2)$ ,  $y_1 (= x_2)$ ,  $a_1 (= a_2 = a_3 = a_4)$ ,  $h_1 (= h_2 = h_3 = h_4)$ ,  $a_5 (= a_6)$ ,  $s_5 (= s_6)$  and  $h_5 (= h_6)$  should be determined. The allowable ranges of these parameter in optimization process are assumed to be  $(0 \sim w/2)$ ,  $(0 \sim w/2)$ ,  $(0.5a \sim a)$ ,  $(0 \sim h+g)$ ,  $(a \sim 3a)$ ,  $(0 \sim w/2)$  and  $(0 \sim h+g)$ , respectively.

The required matching and 3-dB coupling value can be achieved by optimizing the geometric parameters of the

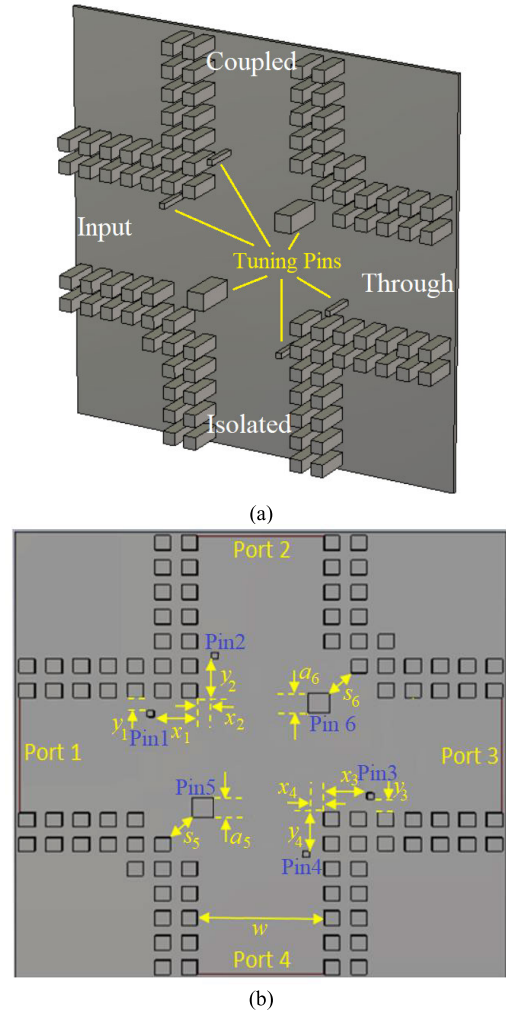


FIGURE 2. Geometry of 3-dB coupler in groove gap waveguide technology. (a) Perspective view. (b) Top view. The top metal plate is not illustrated.

TABLE 1. Optimized values of geometrical parameters of proposed 3-dB directional coupler.

Parameter	$x_1$	$y_1$	$a_1$	$h_1$	$a_5$	$s_5$	$h_5$	$w$
Value (mm)	4.16	1.39	0.66	4.06	3.10	2.13	5.25	12.21

structure. To this end, CST Microwave Studio's optimization tools and time-domain solver are employed in this research. The assumed error function to reach the desired input reflection, low insertion loss, and high isolation is as follows:

$$\text{Error} = \sqrt{\frac{1}{M} \sum_{m=1}^M (|S_{11}(f_m)|^2 + |S_{21}(f_m) + C|^2 + |S_{41}(f_m)|^2)}$$
(1)

where  $C$  is the desired 3-dB coupling value. The optimized values of geometrical parameters are listed in Table 1. Fig. 3 indicates the simulation results for  $S$ -parameters of the couplers. By exciting input port 1, the input reflection falls below -20 dB, and the isolation between ports 1 and 4 exceeds 20 dB.

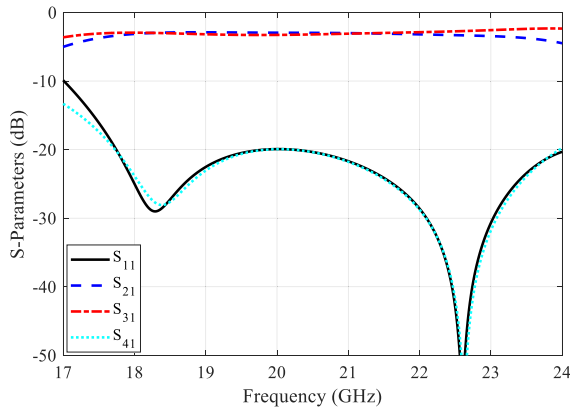


FIGURE 3. S-parameters of 3-dB directional coupler.

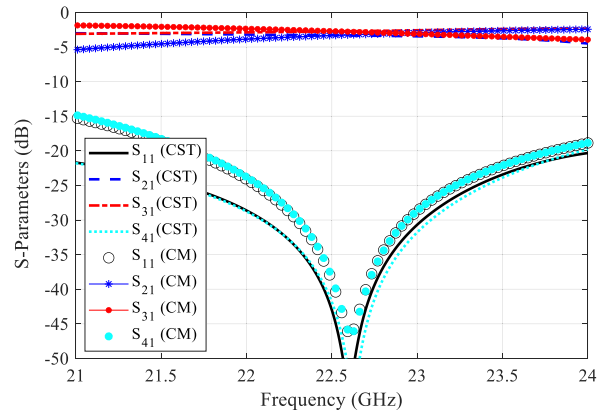


FIGURE 5. Comparison of S-parameters obtained with CST and the circuit model (CM) of 3-dB coupler.

TABLE 2. Optimized values of geometrical parameters of proposed 4.5-, 6-dB and 10-dB directional couplers.

	4.5-dB Coupler	6-dB Coupler	10-dB Coupler
$x_1, y_1, a_1, h_1$	3.22, 0.61, 0.74, 3.69	3.05, 0.70, 0.67, 3.77	1.57, 1.10, 0.59, 3.86
$x_2, y_2, a_2, h_2$	0.94, 1.73, 0.66, 4.28	1.09, 1.57, 0.64, 4.28	2.83, 0.94, 1.62, 5.00
$x_3, y_3, a_3, h_3$	2.40, 0.41, 0.73, 3.75	2.25, 1.09, 0.64, 3.85	1.16, 0.72, 0.63, 5.08
$x_4, y_4, a_4, h_4$	1.13, 5.87, 1.09, 3.15	1.27, 6.2, 1.03, 3.26	1.54, 6.89, 1.90, 3.10
$s_5, a_5, h_5$	4.21, 0.99, 5.05	4.42, 0.73, 5.13	3.65, 0.67, 4.65
$s_6, a_6, h_6$	3.65, 3.31, 5.14	3.27, 1.30, 5.13	3.99, 0.75, 5.13

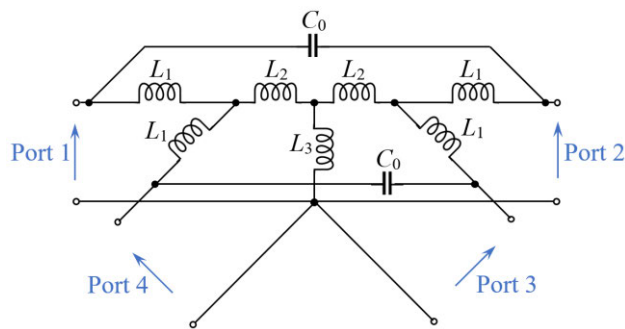


FIGURE 4. Equivalent circuit of loss-less 3-dB directional coupler.

As a result, the transmission coefficients from input to ports 2 and 3 are  $-3 \pm 0.5$  dB from 18 GHz to 24 GHz. By exciting the input port (port 1), the arrangement of tuning pins in the coupling region results in the transfer of approximately half of the input power to port 2 and the other half to port 3, while port 4 is isolated.

### B. CIRCUIT MODEL OF 3-dB DIRECTIONAL COUPLER

The representation of the proposed 3-dB directional coupler in terms of an appropriate, efficient, simple and drawable equivalent circuit is useful from the conceptual design point of view and essential for a better understanding of coupler’s operation. At the same time, the electrical parameters of the equivalent circuit should be easy to identify. Fig 4 present the simplest equivalent circuit of the proposed 3-dB cross-shaped directional coupler. To derive this model, we observe that the coupling region of the proposed GW 3-dB directional coupler resembles a combination of T-junctions. Utilizing circuit models for H-plane three-port waveguide junctions [32], we construct the equivalent circuit, which generally comprises seven inductors and two capacitors. Due to the symmetry and identical nature of all ports in the proposed coupler, the equivalent circuit is simplified to three inductances ( $L_1, L_2$  and  $L_3$ ) and a capacitance  $C_0$ . It is noteworthy that since the behavior of the coupling region including tuning pins is a function of frequency, inductors and capacitors in the proposed equivalent circuit will be frequency dependent and the values of the inductances ( $L_1, L_2$

and  $L_3$ ) and the capacitance  $C_0$  in the simplified model with frequency independent element will depend on the frequency chosen extraction. We decided to extract the elements of the equivalent circuit of the structure at the second resonance frequency of the structure (22.6 GHz). This gives  $L_1 = 0.38$  nH,  $L_2 = 0.27$  nH,  $L_3 = 0.05$  nH,  $C_0 = 0.21$  pF. The S-parameters of the equivalent circuit for the extracted values are depicted in Fig. 5. It is evident that there is a reasonable agreement between the results from the full-wave simulation in CST and circuit model near the resonance frequency of 22.6 GHz.

### C. COUPLERS WITH DESIRED COUPLING LEVEL

By adjusting the dimensions and placement of six tuning pins within the coupling area, it is feasible to achieve the desired coupling level between the input port and the output port while maintaining a compact footprint. For the proof of concept, several other directional couplers have been designed. To achieve low input reflection and insertion loss, and high isolation, the assumed error function expressed in (1) is considered with assuming  $C = 4.5$ -, 6-, and 10-dB.

Briefly, the design procedure of broadband cross-shaped coupler, based on using tuning pins in the coupling region can be expresses as follows:

- First, establish the design frequency at the midpoint of the target bandwidth.
- Next, conduct a gap waveguide design to determine the periodic pin dimensions, ensuring the bandgap encompasses the desired frequency range [12].
- Initially, design a 3-dB coupler by optimizing the structure to determine just seven parameters  $x_1, y_1, a_1, h_1, a_5, s_5$  and  $h_5$ . The allowable ranges of these

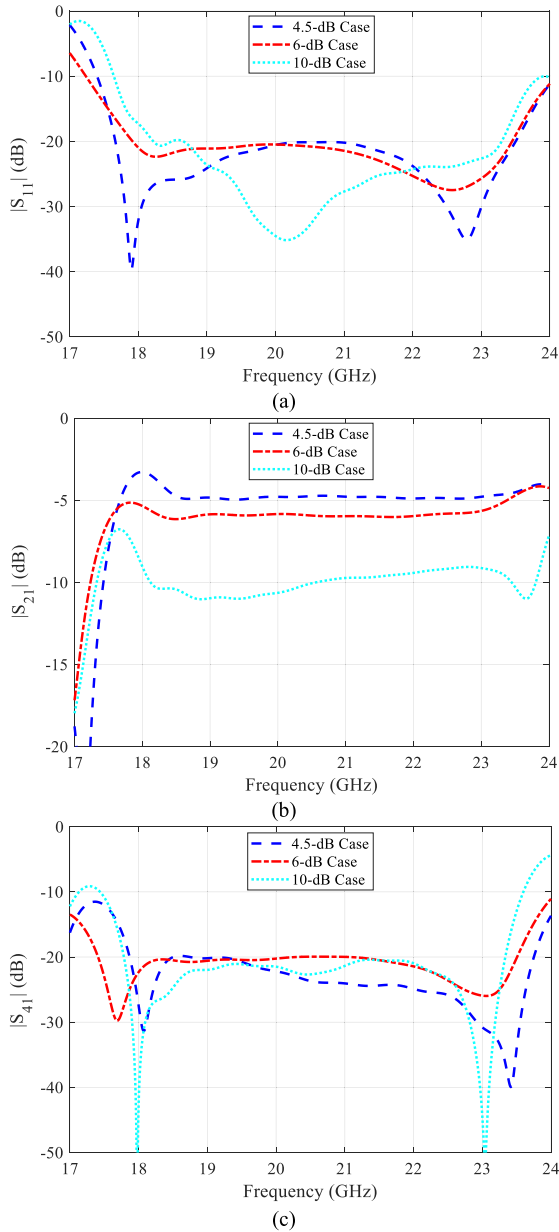


FIGURE 6. S-parameters of 4.5-, 6- and 10-dB directional couplers.

parameter are assumed to be  $(0 \sim w/2)$ ,  $(0 \sim w/2)$ ,  $(0.5a \sim a)$ ,  $(0 \sim h+ag)$ ,  $(a \sim 3a)$ ,  $(0 \sim w/2)$  and  $(0 \sim h+ag)$ , respectively.

- Lastly, use the values obtained from the previous step as the starting point for the geometrical parameters of six pins in the final optimization. Adjust all design variables until the desired coupling and return loss levels are attained.

The optimization is executed on a Windows 10 computational machine with an Intel Xeon Gold 6136 CPU (running at 3.5 GHz, two processors and 36 cores) and 576 GB of RAM. The time consumed for each simulation of the whole structure is less than 30 seconds. The optimized values of geometrical parameters of the structure for different coupling values are listed Table 2.

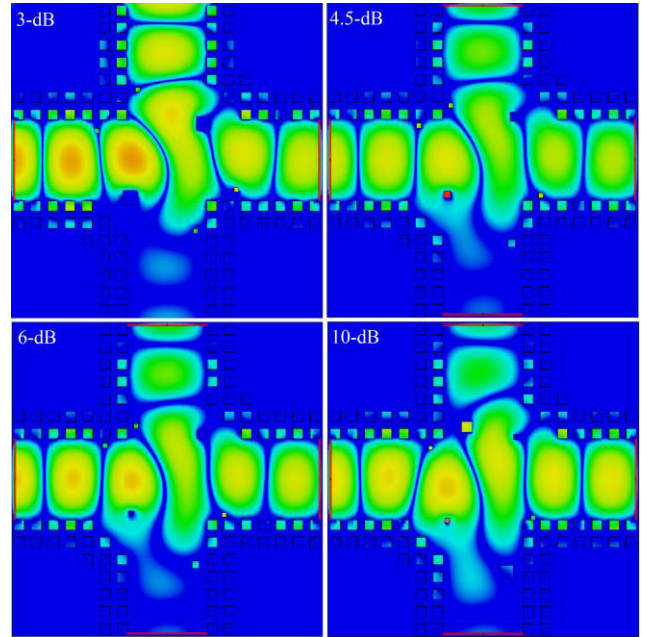


FIGURE 7. Electric field distribution of 3-, 4.5-, 6- and 10-dB directional couplers at 21 GHz.

The simulation results for S-parameters of the designed couplers are depicted in Fig. 6. According the results, the input reflection coefficients are below  $-15$  dB, and the isolation values between ports 1 and 4 are higher than 15 dB over the frequency range from 17.8 GHz to 23.5 GHz. As a result, the transmission coefficient from input to port 2 in three designed couplers are  $-4.5 \pm 0.5$  dB,  $-6 \pm 0.5$  dB, and  $-10 \pm 1$  dB, respectively. One can find that the simulation results confirm that the directional couplers effectively achieve the intended power distribution across the output ports. It is feasible to design a coupler that exhibits wide-band capabilities, satisfactory coupling flatness, and coupling values ranging from 3 dB to 10 dB. The electric field distributions of the proposed directional couplers at 21 GHz are displayed in Fig. 7 to prove their performances.

#### IV. COMPLETE 3-dB DIRECTIONAL COUPLER

##### A. DESIGN OF TRANSITION

The integration of the proposed coupler with standard flange waveguides is achieved through transitions between the groove gap waveguide and the standard WR-42 rectangular waveguide. Fig. 8 depicts the transition design, which extends the groove waveguides to align with the output waveguide ports and incorporates stepped metal bricks near the apertures.

To design this transition, a dual back-to-back transition structure is utilized. The optimization of geometrical parameters is essential to convert the groove gap waveguide mode into the rectangular waveguide's dominant mode effectively. This optimization ensures proper matching at the input port and minimizes insertion loss across the desired frequency spectrum. The optimized values (in mm) are as follows  $l_{t1} =$

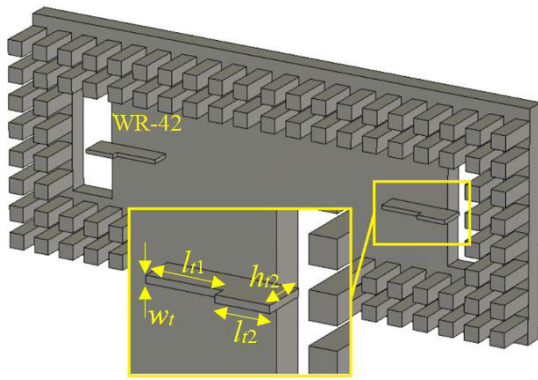


FIGURE 8. Geometry of back-to-back transitions from groove gap waveguide to WR-42.

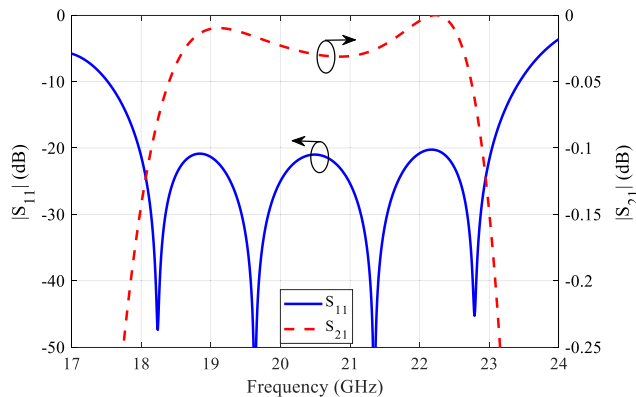


FIGURE 9. S-parameters of back-to-back transitions from groove gap waveguide to WR-42.

4.11,  $l_{t2} = 2.92$ ,  $h_{t1} = 2.00$ ,  $h_{t2} = 2.68$  and  $w_t = 0.41$ . The simulation results for the S-parameters of the optimized structure are shown in Fig. 9. The input reflection coefficient of the structure is less than -20 dB and the transmission loss is less than 0.1 dB from 18 to 23 GHz.

**B. CONFIGURATION OF COMPLETE COUPLER**

The complete configuration of proposed 3-dB coupler including coupling region, groove gap waveguides and transitions from groove gap waveguide to standard WR-42 rectangular waveguide is displayed in Fig. 10. Here, the goal is to minimize the overall dimensions of the coupler with the addition of transitions. Therefore, according to the dimensions of the standard WR-42 adapters (as shown in Fig. 10(b)), the transitions are located at the shortest possible distance from the coupling area, which causes multiple wave reflections between the transitions and the coupling region. In this case, the whole structure is re-optimized so that these effects are reduced as much as possible and the desired input reflection coefficient, isolation and coupling coefficient are obtained in the desired bandwidth. The final values of geometrical parameter for the 3-dB directional coupler (in mm) are given in Table 3.

The impact of different parameters on the transition performance from the groove gap waveguide to WR-42 is assessed

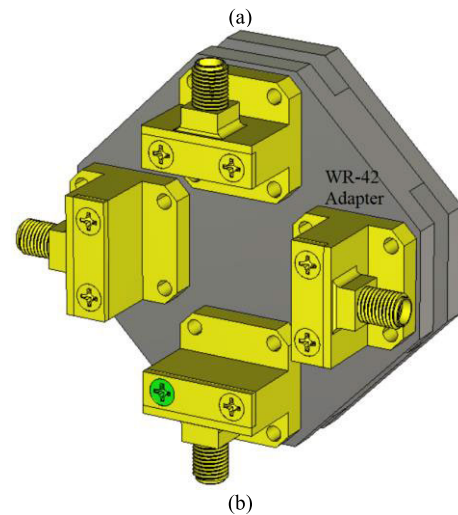
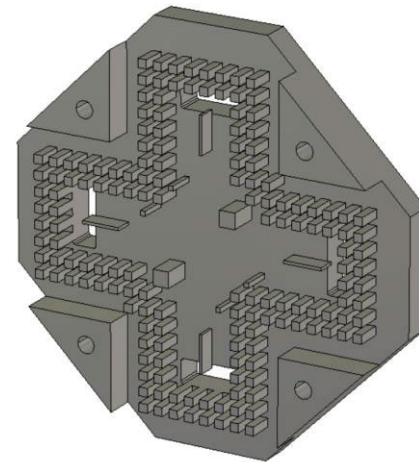


FIGURE 10. The geometry of complete 3-dB coupler with groove gap waveguides to WR-42 transition. (a) Top view. (b) back view.

TABLE 3. Optimized values of geometrical parameters of complete 3-dB directional coupler with four transitions.

Parameter	$x_1$	$y_1$	$a_1$	$h_1$	$a_5$	$s_5$	$h_5$	$w_t$	$h_t$	$l_t$
Value (mm)	2.73	1.47	0.66	5.00	5.86	2.25	5.19	0.50	3.09	6.58

by performing numerous simulations with varying values for  $w_t$ ,  $l_t = l_{t1} + l_{t2}$ , and  $h_t = h_{t1} = h_{t2}$ . As depicted in Fig. 11, the dimensions of the metal brick section significantly affect the input reflection coefficient.

**V. FABRICATION AND MEASUREMENT**

To experimentally validate our design, we selected a 3-dB directional coupler as our prototype. Fabrication was carried out using low-loss aluminum on a SPINNER CNC machine, ensuring accuracy within 12  $\mu\text{m}$  and surface smoothness of up to 0.8  $\mu\text{m}$ . The image of this manufactured device can be seen in Fig. 12. The overall size of the structure, including flange connections, is 50 mm  $\times$  50 mm  $\times$  10 mm.

For S-parameter measurements, we employed an Agilent 8722ES vector network analyzer. Thru-reflect-line (TRL) calibration was utilized to account for the influence of coax to WR-42 waveguide adapters in the calibration process.

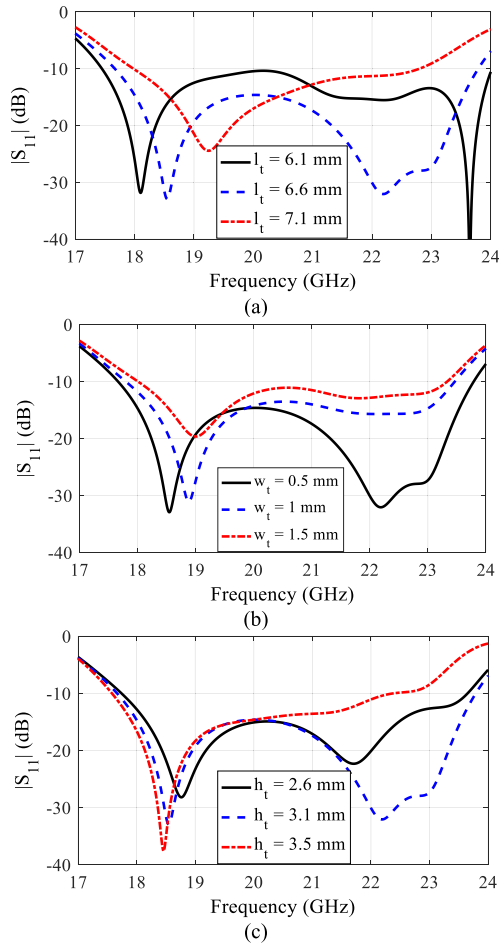


**FIGURE 11.**  $|S_{11}|$  of 3-dB coupler with different values of  $l_t, w_t$  and  $h_t$  of the groove gap waveguide to WR-42 transition.

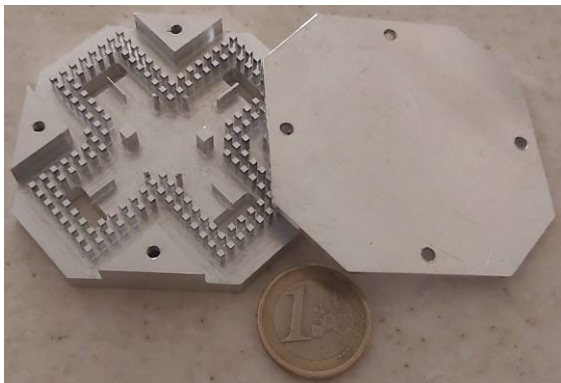


**FIGURE 12.** The photograph of the sample 3-dB directional coupler.

Fig. 13 compares the measurement results with simulations for the input reflection coefficient, port to port coupling, and phase difference between the output ports. As can be noticed, the measured input reflection coefficient and the isolation among ports 1 and 4 are better than 15 dB over the 18-23.7 GHz frequency range. The observed operational frequency band aligns closely with the simulated operational frequency band. Minor discrepancies between the simulation and measurement results may be attributed to fabrication tolerances and the connection of waveguide adaptors. According

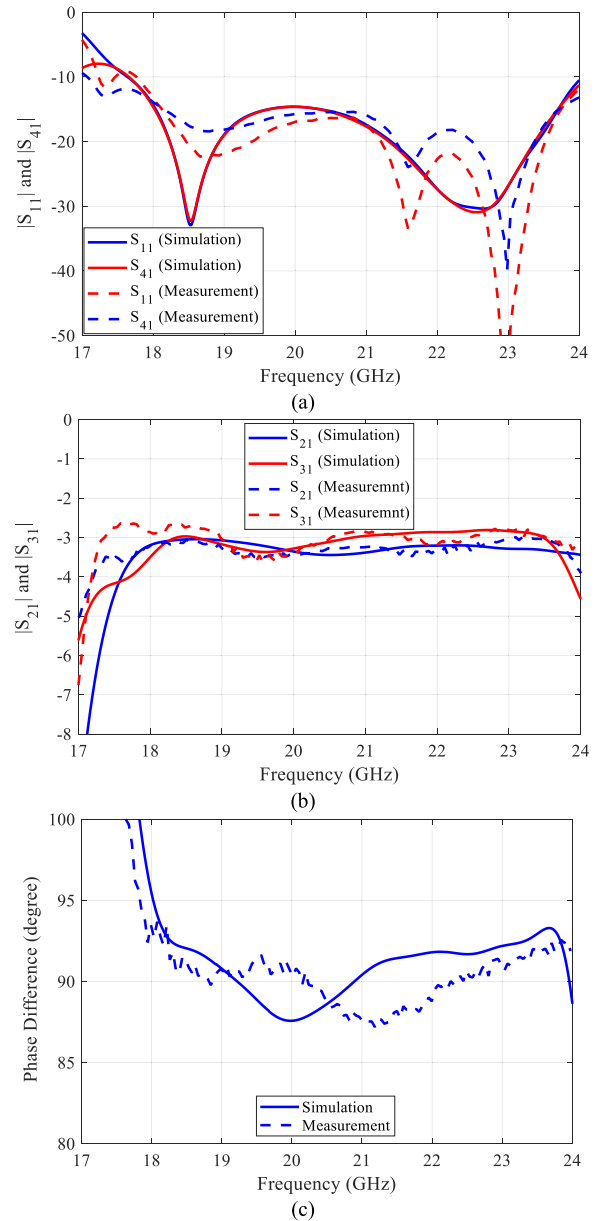


**FIGURE 13.** Simulated and measured S-parameters of the proposed 3-dB directional coupler.

to the measurement results, the amplitude imbalance between ports 2 and 3 is within  $\pm 0.5$  dB, and the phase imbalance is below  $\pm 2.5^\circ$  over the 17.9-24 GHz band. The measurement results confirm that the power distribution between the output ports corresponds to a 3-dB hybrid directional coupler.

Table 4 compares the performance of several reported PCB- and gap waveguide-based 3-dB couplers with the present work. It should be noted that while PCB-based couplers [2], [3], [21], [22], [23], [24], [25] may offer relatively wide frequency bandwidth and low profile, and can be manufactured using a cost-effective conventional process, they are not suitable for high-power applications. In contrast to other reported works employing metal ridge and groove gap waveguides, our proposed coupler is self-packaged and exhibits

TABLE 4. Comparison with other reported 3-dB couplers.

Ref.	Technology	Center Frequency (GHz)	Bandwidth ( $S_{11} < -10$ dB)	Amplitude Balance (dB) BW ( $\pm 0.5$ dB)	Phase Balance (degree) BW ( $\pm 5^\circ$ )	Coupling Region Size ( $\lambda_g \times \lambda_g$ )	Power Handling
[2]	SIW	24	18%	-4.7 $\pm$ 0.5 BW = 18%	92 $\pm$ 2 BW = 18%	1.3 $\times$ 1.1	Low
[3]	Microstrip	30	11.2%	-3 $\pm$ 0.5 BW = 11.2%	90 $\pm$ 1 BW = 11.2%	1.5 $\times$ 1.5	Low
[21]	SIGW	26.2	20%	3.7 $\pm$ 0.5 BW = 20%	90 $\pm$ 3 BW = 20%	1.8 $\times$ 1.6	Low
[22]	PRGW	30	6%	-3.6 $\pm$ 1 BW = 3%	90 $\pm$ 10 BW = 3%	1.1 $\times$ 1.1	Low
[23]	PRGW	30	26.5%	-3.6 $\pm$ 0.75 BW = 10%	90 $\pm$ 5 BW = 23%	2 $\times$ 2	Low
[24]	PRGW	30	13%	-3.7 $\pm$ 0.8 BW = 6.7%	90 $\pm$ 10 BW = 7%	1.12 $\times$ 1.12	Low
[25]	PRGW	30	26.5%	-3.6 $\pm$ 0.75 BW = 10%	90 $\pm$ 5 BW = 26.5%	2 $\times$ 2	Low
[26]	PRGW	30	38%	-3.4 $\pm$ 0.5 BW = 26.5%	90 $\pm$ 5 BW = 38%	1.3 $\times$ 1.3	Low
[27]	RGW	15.5	14%	-3 $\pm$ 1 BW = 7%	N.A	1.6 $\times$ 1.6	High
[28]	GGW	14	14.3%	-3.25 $\pm$ 0.75 BW = 13%	90 $\pm$ 0.75 BW = 14.3%	3 $\times$ 2	High
[31]	RGW	16	50%	-3 $\pm$ 0.7 BW = 50%	91 $\pm$ 3 BW = 50%	2.2 $\times$ 1.7	High
[16]	RGW	30	13%	-3 $\pm$ 0.8 BW = 11%	90 $\pm$ 2 BW = 13%	3 $\times$ 1.5	High
This Work	GGW	20.5	29.1%	-3 $\pm$ 0.5 dB BW = 29.1%	89.5 $\pm$ 2.5 BW = 29.1%	1.2 $\times$ 1.2	High

GGW: Groove Gap Waveguide, RGW: Ridge Gap Waveguide, PRGW: Printed Ridge Gap Waveguide.

satisfactory performance in terms of wide bandwidth, amplitude and phase balance, low loss, and coupling flatness. Unlike designs that require a coupling region spanning several wavelengths ( $\lambda_g$ ) to achieve the performance detailed in Table 4, the presented coupler accomplishes comparable performance with a smaller coupling region size of  $1.2 \lambda_g \times 1.2 \lambda_g$ . This performance level combined with compactness and simple construction offers a significant advantage, particularly in high-frequency bands where the fabrication of devices based on hollow waveguides presents significant challenges.

## VI. CONCLUSION

A compact broad band groove gap waveguide-based 3-dB directional coupler for Ka-band is presented. The fabrication problem in high frequency bands is solved by employing gap waveguide technique. The fabricated sample exhibits coupling values of  $3 \pm 0.5$  dB in the output ports with phase imbalance of  $\pm 2.5^\circ$  over the 17.9-24 GHz frequency band. The design presented here provides a significantly broader operational band compared to most other reported 3dB gap waveguide couplers. It also demonstrates high isolation between the input and isolated ports, all while preserving a compact form factor. The proposed 3-dB directional coupler can be used in feeding networks of array antennas and power combing networks of microwave systems.

## REFERENCES

- [1] S. B. Cohn and R. Levy, "History of microwave passive components with particular attention to directional couplers," *IEEE Trans. Microw. Theory Techn.*, vol. MTT-32, no. 9, pp. 1046–1054, Sep. 1984.
- [2] T. Djerfai and K. Wu, "Super-compact substrate integrated waveguide cruciform directional coupler," *IEEE Microw. Wireless Compon. Lett.*, vol. 17, no. 11, pp. 757–759, Nov. 2007.
- [3] X. F. Ye, S. Y. Zheng, and Y. M. Pan, "A compact millimeter-wave patch quadrature coupler with a wide range of coupling coefficients," *IEEE Microw. Wireless Compon. Lett.*, vol. 26, no. 3, pp. 165–167, Mar. 2016.
- [4] X. Jin, Z. Liu, Y. Xiao, and Z. Chen, "Design and error analysis of W-band SIW cruciform directional coupler," in *Proc. IEEE 11th Asia-Pacific Conf. Antennas Propag. (APCAP)*, Guangzhou, China, Nov. 2023, pp. 1–2, doi: 10.1109/APCAP59480.2023.10470126.
- [5] H. Oraizi, "Optimum design of multihole directional couplers with arbitrary aperture spacing," *IEEE Trans. Microw. Theory Techn.*, vol. 46, no. 4, pp. 331–342, Apr. 1998.
- [6] Y. Zhang, Q. Wang, and H. Xin, "A compact 3 dB E-plane waveguide directional coupler with full bandwidth," *IEEE Microw. Wireless Compon. Lett.*, vol. 24, no. 4, pp. 227–229, Apr. 2014.
- [7] N. J. G. Fonseca and J.-C. Angevain, "Waveguide hybrid septum coupler," *IEEE Trans. Microw. Theory Techn.*, vol. 69, no. 6, pp. 3030–3036, Jun. 2021.
- [8] R. Levy, "Analysis of practical branch-guide directional couplers (correspondence)," *IEEE Trans. Microw. Theory Techn.*, vol. MTT-17, no. 5, pp. 289–290, May 1969.
- [9] T. Shen, K. A. Zaki, and T. Dolan, "Waveguide branch couplers for tight couplings," in *IEEE MTT-S Int. Microw. Symp. Dig.*, Jun., pp. 1319–1322.
- [10] Z. Niu, B. Zhang, K. Yang, Y. Yang, D. Ji, Y. Liu, Y. Feng, Y. Fan, X. Chen, and D. Li, "Mode analyzing method for fast design of branch waveguide coupler," *IEEE Trans. Microw. Theory Techn.*, vol. 67, no. 12, pp. 4733–4740, Dec. 2019.
- [11] B. Dai, B. Zhang, Z. Niu, Y. Feng, Y. Liu, and Y. Fan, "A novel ultrawideband branch waveguide coupler with low amplitude imbalance," *IEEE Trans. Microw. Theory Techn.*, vol. 70, no. 8, pp. 3838–3846, Aug. 2022.
- [12] A. U. Zaman and P.-S. Kildal, "GAP waveguides," in *Handbook of Antenna Technologies*. Singapore: Springer, 2016.
- [13] A. Farahbakhsh, "Ka-band coplanar magic-T based on gap waveguide technology," *IEEE Microw. Wireless Compon. Lett.*, vol. 30, no. 9, pp. 853–856, Sep. 2020.
- [14] A. Karami Horestani, Z. Shaterian, and M. Mrozowski, "Low-loss mechanically tunable resonator and phase shifters in groove gap waveguide technology," *IEEE Access*, vol. 10, pp. 70964–70970, 2022.
- [15] S. Peng, Y. Pu, Z. Wu, and Y. Luo, "High-isolation power divider based on ridge gap waveguide for broadband millimeter-wave applications," *IEEE Trans. Microw. Theory Techn.*, vol. 70, no. 6, pp. 3029–3039, Jun. 2022.
- [16] D. Zarifi, A. Farahbakhsh, and A. U. Zaman, "A millimeter-wave six-port junction based on ridge gap waveguide," *IEEE Access*, vol. 11, pp. 68699–68705, 2023.



- [17] A. K. Horestani and M. Mrozowski, "A wideband rotary-joint-free H-plane horn antenna with 360° steerable radiation pattern using gap waveguide technology," *IEEE Trans. Antennas Propag.*, vol. 71, no. 7, pp. 5717–5728, Jul. 2023.
- [18] B. Yao, N. Huang, G. Zhang, X. Zhou, J. Lu, K. W. Tam, W. Zhang, and W. Tang, "Dual-band bandpass filter with high selectivity based on 3D printable groove gap waveguide," *IET Microw., Antennas Propag.*, vol. 17, no. 10, pp. 827–831, Aug. 2023.
- [19] Z.-H. Shi, F. Wei, L. Yang, and R. Gómez-García, "High-selectivity inverted microstrip gap waveguide bandpass filter using hybrid cavity and stub-loaded ring resonant modes," *IEEE Trans. Circuits Syst. II, Exp. Briefs*, vol. 71, no. 1, pp. 146–150, Jan. 2024.
- [20] M. Farahani, M. Akbari, M. Nedil, T. A. Denidni, and A. R. Sebak, "A novel low-loss millimeter-wave 3-dB 90° ridge-gap coupler using large aperture progressive phase compensation," *IEEE Access*, vol. 5, pp. 9610–9618, 2017.
- [21] D. Shen, K. Wang, and X. Zhang, "A substrate integrated gap waveguide based wideband 3-dB coupler for 5G applications," *IEEE Access*, vol. 6, pp. 66798–66806, 2018.
- [22] M. M. M. Ali, S. I. Shams, and A.-R. Sebak, "Printed ridge gap waveguide 3-dB coupler: Analysis and design procedure," *IEEE Access*, vol. 6, pp. 8501–8509, 2018.
- [23] M. M. M. Ali, S. I. Shams, and A. Sebak, "Ultra-wideband printed ridge gap waveguide hybrid directional coupler for millimetre wave applications," *IET Microw., Antennas Propag.*, vol. 13, no. 8, pp. 1181–1187, Jul. 2019.
- [24] Z. Zhao and T. A. Denidni, "Millimeter-wave printed-RGW hybrid coupler with symmetrical square feed," *IEEE Microw. Wireless Compon. Lett.*, vol. 30, no. 2, pp. 156–159, Feb. 2020.
- [25] M. M. M. Ali, M. S. El-Gendy, M. Al-Hasan, I. B. Mabrouk, A. Sebak, and T. A. Denidni, "A systematic design of a compact wideband hybrid directional coupler based on printed RGW technology," *IEEE Access*, vol. 9, pp. 56765–56772, 2021.
- [26] M. M. M. Ali, O. M. Haraz, I. Afifi, A.-R. Sebak, and T. A. Denidni, "Ultra-wideband compact millimeter-wave printed ridge gap waveguide directional couplers for 5G applications," *IEEE Access*, vol. 10, pp. 90706–90714, 2022.
- [27] S. I. Shams and A. A. Kishk, "Design of 3-dB hybrid coupler based on RGW technology," *IEEE Trans. Microw. Theory Techn.*, vol. 65, no. 10, pp. 3849–3855, Oct. 2017.
- [28] D. Zarifi and A. R. Shater, "Design of a 3-dB directional coupler based on groove gap waveguide technology," *Microw. Opt. Technol. Lett.*, vol. 59, no. 7, pp. 1597–1600, Jul. 2017.
- [29] M. Nasri, D. Zarifi, and A. U. Zaman, "A wideband 3-dB directional coupler in GGW for use in V-Band communication systems," *IEEE Access*, vol. 8, pp. 17819–17823, 2020.
- [30] M. Taraji and M. Naser-Moghaddasi, "Design of branch line coupler based on ridge gap waveguide technology for X-band application," *IETE J. Res.*, vol. 68, no. 2, pp. 917–923, Mar. 2022.
- [31] P. Mahdavi, S. E. Hosseini, and P. Shojaadini, "Broadband three-section branch-line coupler realized by ridge gap waveguide technology from 12 to 20 GHz," *IEEE Access*, vol. 11, pp. 46903–46914, 2023.
- [32] N. Marcuvitz, "Microwave networks," in *Waveguide Handbook*, vol. 10. London, U.K.: The Institution of Engineering and Technology, 1986, pp. 101–167.



**MAHDIEH RABBANIFARD** was born in Kashan, Iran, in 1991. She received the B.Sc. degree in electrical engineering from the Azad University of Kashan, Kashan, in 2015. She is currently pursuing the M.Sc. degree in electrical engineering with the University of Kashan, Iran. Her current research interests include gap waveguide technology, antenna design, and microwave components.



**DAVOOD ZARIFI** was born in Kashan, Iran, in 1987. He received the B.S. degree in electrical engineering from the University of Kashan, Kashan, in 2009, and the M.S. and Ph.D. degrees in electrical engineering from Iran University of Science and Technology (IUST), Tehran, Iran, in 2011 and 2015, respectively. He is currently an Associate Professor with the School of Electrical and Computer Engineering, University of Kashan. He is also a Guest Associate Professor with Gdańsk University of Technology, Gdańsk, Poland, hosted by Prof. Michal Mrozowski. His research interests are applications of metamaterials, microwave passive components, slot array antennas, and gap waveguide technology.



**ALI FARAHBAKSH** was born in Kerman, Iran, in 1984. He received the Ph.D. degree in electrical engineering from Iran University of Science and Technology, Tehran, Iran, in 2016. He is currently an Associate Professor with the Department of Electrical and Computer Engineering, Graduate University of Advanced Technology, Kerman. He is also a Guest Associate Professor with Gdańsk University of Technology, Gdańsk, Poland, hosted by Prof. Michal Mrozowski. His research interests include microwave and antenna engineering, including gap waveguide technology, millimeter-wave high-gain array antenna, microwave devices, electromagnetic wave propagation and scattering, inverse problems in electromagnetic, and anechoic chamber design.



**MICHAL MROZOWSKI** (Fellow, IEEE) received the M.Sc. degree (Hons.) in telecommunication engineering and the Ph.D. degree (Hons.) in electronic engineering from Gdańsk University of Technology (GUT), in 1983 and 1990, respectively. In 1986, he joined the Department of Electronics, GUT, where he is currently a Full Professor, the Head of the Department of Microwave and Antenna Engineering, and the Director of the Doctoral School. He has developed several software modules that have been then integrated into commercial microwave EDA software used all over the world. He has published one book and over 100 peer-reviewed articles in IEEE journals. His research interests include computational electromagnetics, photonics, and microwave engineering. His current work is focused on the development of new fast numerical techniques for solving 2D and 3D boundary value problems in the time and frequency domains, automated microwave filter design, microwave filter synthesis, microwave sensor design, microwave EDA, reduced-order models for grid-based numerical techniques (e.g., FDTD and FEM), and surrogate model construction. He also serves as a member of the editorial board for IEEE ACCESS. He is a member of the MTT-1 and MTT-2 Technical Committees, a fellow of the Electromagnetics Academy, and a member of the Polish Academy of Sciences. Furthermore, he is the Past Vice-Dean of Research of the ETI Faculty and the Past Chairperson of the Polish AES/AP/MTT Chapter. He served as an Associate Editor for IEEE MICROWAVE AND WIRELESS COMPONENTS LETTERS and a member of the editorial board for PROCEEDINGS OF THE IEEE.

• • •